iScience

CellPress
OPEN ACCESS

Article

# Non-Omicron breakthrough infection with higher viral load and longer vaccination-infection interval improves SARS-CoV-2 BA.4/5 neutralization

Sho Miyamoto,[1,6] Takeshi Arashiro,[1,2,6] Akira Ueno,[1] Takayuki Kanno,[1] Shinji Saito,[1] Harutaka Katano,[1] Shun Iida,[1] Akira Ainai,[1] Seiya Ozono,[1] Takuya Hemmi,[1] Yuichiro Hirata,[1] Saya Moriyama,[3] Ryutaro Kotaki,[3] Hitomi Kinoshita,[4] Souichi Yamada,[4] Masaharu Shinkai,[5] Shuetsu Fukushi,[4] Yoshimasa Takahashi,[3] and Tadaki Suzuki[4,7,*]

## SUMMARY

**The immune responses to SARS-CoV-2 variants in COVID-19 cases are influenced by various factors including pre-existing immunity via vaccination and prior infection. Elucidating the drivers for upgrading neutralizing activity to SARS-CoV-2 in COVID-19 cases with pre-existing immunity will aid in improving COVID-19 booster vaccines with enhanced cross-protection against antigenically distinct variants, including the Omicron sub-lineage BA.4/5. This study revealed that the magnitude and breadth of neutralization activity to SARS-CoV-2 variants after breakthrough infections are determined primarily by upper respiratory viral load and vaccination-infection time interval. Extensive neutralizing breadth, covering even the most antigenically distant BA.4/5, was observed in cases with higher viral load and longer time intervals. Antigenic cartography depicted a critical role of the time interval in expanding the breadth of neutralization to SARS-CoV-2 variants. Our results illustrate the importance of dosing interval optimization as well as antigen design in developing variant-proof booster vaccines.**

## INTRODUCTION

The proportion of individuals in the population with antiviral immunity to severe acute respiratory syndrome coronavirus type 2 (SARS-CoV-2) has increased dramatically due to the ongoing pandemic of coronavirus disease 2019 (COVID-19) and extensive worldwide COVID-19 vaccine campaigns. Nevertheless, COVID-19 cases continue to increase, causing significant morbidity and mortality worldwide, due to the emergence of variants of concern (VOCs) with varying levels of increased transmissibility and resistance to existing immunity; thus, highlighting the necessity to develop next-generation COVID-19 booster vaccines. These vaccines must induce a durable and broad breadth of protective immunity covering all SARS-CoV-2 variants.[1] Many open questions remain about how to induce high-quality immunity that suppresses viruses with distinct antigenicity. A better understanding of immune responses to SARS-CoV-2 variants infection will ultimately yield better vaccine designs.

The most recently emerged VOC, the Omicron (B.1.1.529 lineage) variant, has spread rapidly worldwide at an unprecedented pace and with rapidly expanding viral genome diversity (World Health Organization (WHO), https://www.who.int/publications/m/item/weekly-epidemiological-update-on-covid-19—8-march-2022). The Omicron BA.1 is characterized by approximately 30 amino acid mutations, three short deletions, and one insertion in the spike protein; 15 mutations are located in the receptor-binding domain (RBD) and induce evasion of humoral immunity induced by prior infection or vaccination.[2–4] Despite the high capability for humoral immunity evasion seen in BA.1, cross-neutralizing activity against BA.1 is elicited in booster vaccinees.[2,5,6] Research groups, including our own, have reported that cross-neutralizing activity against BA.1 is elicited in COVID-19 vaccine breakthrough infections.[7–10] However, the BA.2 sub-lineages account for the main Omicron sub-lineages as of June 2022, and the proportion of BA.4 and BA.5 sub-lineages has been continuously increasing globally since July 2022 (WHO, https://www.who.int/publications/m/item/weekly-epidemiological-update-on-covid-19—22-june-2022). BA.2, which differs from BA.1 in 11 spike protein mutations, significantly changes the ability of the virus to evade immunity.[11–13]

[1]Department of Pathology, National Institute of Infectious Diseases, Tokyo 162-8640, Japan

[2]Center for Surveillance Immunization and Epidemiologic Research, National Institute of Infectious Diseases, Tokyo 162-8640, Japan

[3]Research Center for Drug and Vaccine Development, National Institute of Infectious Diseases, Tokyo 162-8640, Japan

[4]Department of Virology I, National Institute of Infectious Diseases, Tokyo 162-8640, Japan

[5]Tokyo Shinagawa Hospital, Tokyo 140-8522, Japan

[6]These authors contributed equally

[7]Lead contact

*Correspondence: tksuzuki@niid.go.jp

https://doi.org/10.1016/j.isci.2023.105969


This is an open access article under the CC BY-NC-ND license (http://creativecommons.org/licenses/by-nc-nd/4.0/).

As compared to BA.2, BA.4 and BA.5 share some mutations on their spike protein, including the 69/70 deletion, L452R, and F486V, which have been linked to enhanced immune evasion capabilities against the serum from being vaccinated 3 times.[14–16] This poses a major public health concern and could cause an upcoming COVID-19 case upsurge.

Notably, convalescent sera from patients with breakthrough infections show more variable neutralizing antibody titers against Omicron sub-lineages than in those receiving booster vaccinations.[14–18] Moreover, the time interval from vaccination to infection determines the induction of cross-neutralization to BA.1 variants; a longer interval contributes to greater induction of cross-neutralizing antibodies.[7,19] In addition, it has been reported that a long dose interval between the first and second shots induces higher neutralizing and spike-binding antibodies to non-Omicron VOCs and Omicron BA.1 compared to standard dose interval.[20–22] In contrast to a booster vaccination, where both the dose and interval between vaccinations are controlled, the time interval between vaccination and breakthrough infection is not controlled resulting in diverse humoral immune responses against SARS-CoV-2 variants in breakthrough infections. However, other factors, such as symptoms, the infected viral strain, and viral replication, are expected to impact the immune response to SARS-CoV-2 infection. Primary drivers of humoral immune responses to SARS-CoV-2 in breakthrough infections have not been fully elucidated. Research in this area will provide fundamental insights which will contribute to better vaccine designs, especially for booster vaccines.

We evaluated the relationships between the amount of cross-neutralization activity to SARS-CoV-2 variants including Omicron BA.1, BA.2, and BA.4/5 sub-lineage viruses at acute and convalescent phases, upper respiratory tract viral load, and vaccination-infection time interval in non-Omicron breakthrough infection, as well as other case characteristics, and identified the key drivers of the magnitude and breadth of neutralization potency to SARS-CoV-2 variants in individuals with pre-existing immunity against SARS-CoV-2 due to combinations of vaccination and breakthrough infection.

## RESULTS

### Upper respiratory viral load and serum cross-neutralizing activity

We performed virological characterization of 220 breakthrough SARS-CoV-2 infected individuals, diagnosed 14 days after their second vaccination, using upper respiratory specimens collected within four days after diagnosis or disease onset (interquartile range; 0-0 days) (Tables S1 and S2). Spike-mutation detection polymerase chain reaction (PCR) and viral genome analysis showed that most infected viruses were Delta or Alpha variants (Table S1). Viral RNA loads and infectious viral titers in upper respiratory specimens were significantly higher in Delta-infected individuals than in Alpha-infected individuals (Figure 1A). Viral RNA loads and infectious viral titers were positively correlated with the same extent in both variants (Figure S1A), suggesting no difference in the relationship between infectious viral amount and viral RNA levels between the variants. These results suggest that the Delta variant replicates more efficiently in the upper respiratory tract in breakthrough-infected individuals, consistent with previous reports.[23,24]

Sera from the enrolled cases were also obtained at one or two additional time points after infection. We defined the acute phase as within four days after diagnosis (four days after onset for cases diagnosed after onset) and the convalescent phase was defined as seven days after diagnosis or onset, based on the dynamics of anti-spike (S) RBD and anti-nucleoprotein (N) antibody titers (Figures S1B and S1C). We considered cases with positive anti-N antibody titers in the acute phase to have a history of pre-existing infection. Only two cases with a history of a previous infection were included in our study, and the anti-S antibody titers in these cases during the convalescent phase were comparable to those of breakthrough infection cases with no history of previous infection (Figure S1B). Additionally, cases with acute phase anti-S RBD antibody titers <10 U/mL were excluded from this analysis because they were considered as low responders to COVID-19 vaccination. Following this, 26 cases with sera collected in the acute phase and 51 cases with sera collected in the convalescent phase (16 of whom had both acute and convalescent-phase sera) were enrolled for further analysis. Serum-neutralizing activity in these cases was measured using pseudovirus- or live virus-based assays (Figures 1B and S1D). Neutralization titers to the ancestral and BA.2 viruses were strongly correlated (Figure S1E). Neutralization titers determined by pseudovirus-based assays were used for further analyses.

Neutralizing activity for all variants was higher in the convalescent phase than in the acute phase. (Figures 1B and S1D). Acute phase sera showed lower neutralizing activity to Beta, Delta, BA.1, BA.2,

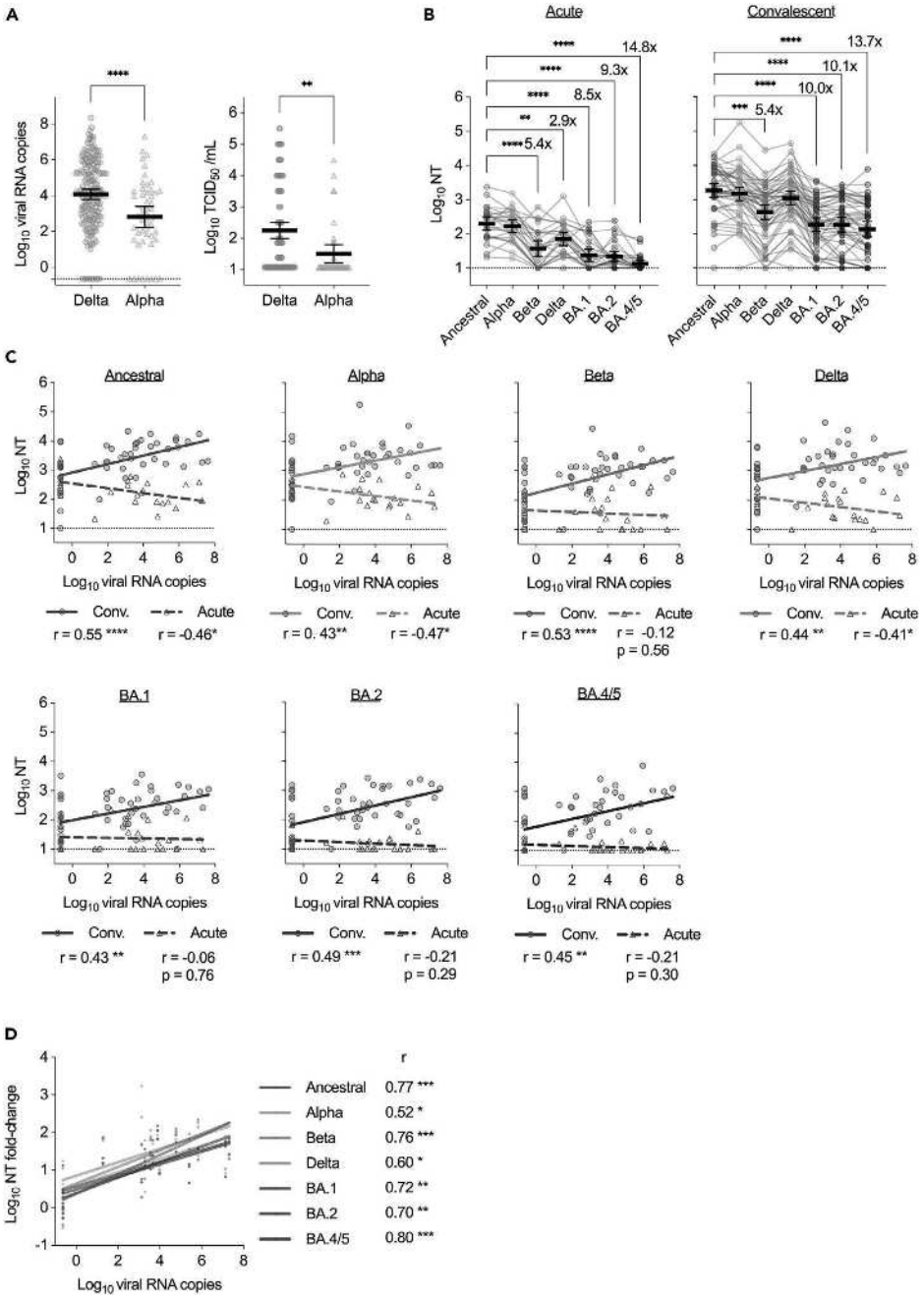


**Figure 1. Relationship between serum neutralization titers and upper respiratory viral load in vaccine breakthrough SARS-CoV-2 infections**

(A) Viral load in respiratory specimens at a near-diagnosis date. Viral RNA copies/reaction and viral titers for cases of SARS-CoV-2 Delta or Alpha variant infection were measured using reverse transcription qPCR (RT-qPCR; left) and the median tissue culture infectious dose ($TCID_{50}$; right), respectively. Viral titers are shown in viral isolation-positive cases. Mean ±95% confidence intervals (CIs) are presented. Viral loads were compared using unpaired t-tests.

(B) Neutralization titers (NTs) in vaccine breakthrough case sera against SARS-CoV-2 pseudoviruses at acute and convalescent phases. Data from the same serum are connected with lines. Mean ±95% CIs are presented for each serum

**Figure 1. *Continued***
titer. Titers between ancestral and newer variants were compared using ANOVA with Dunnett's test. Fold reductions are indicated above the columns.
(C) Correlations between viral load in respiratory specimens at the near-diagnosis date and neutralization titers against the indicated variant at acute and convalescent phases.
(D) Correlations between viral load and fold-changes in neutralization titers in acute and convalescent phases. (C and D) show regression lines, Pearson correlation r values, and significance levels. Statistical significance: *p < 0.05, **p < 0.01, ***p < 0.001, ****p < 0.0001. Dotted lines indicate cutoff values.

and BA.4/5 viruses than to ancestral strain, and more than half of the neutralizing titers to BA.4/5 virus were below the detection limit. Convalescent-phase sera showed lower neutralizing activity to Beta, BA.1, BA.2, and BA.4/5 viruses than to the ancestral strain. Notably, no obvious differences were found in the neutralizing activity among BA.1, BA.2, and BA.4/5 viruses in convalescent-phase sera, suggesting negligible antigenic difference among Omicron sub-lineages in non-Omicron breakthrough sera. Acute and convalescent neutralization titers were lower to BA.2 than to ancestral strain (using live virus-based assays) (Figure S1D), which confirmed the results obtained in the pseudoviruses-based assay. Convalescent-phase sera from Delta breakthrough infections showed higher neutralizing activity against ancestral and Beta variants than sera from Alpha breakthrough infections, and both demonstrated equivalent neutralizing activity against Alpha and Delta viruses. No apparent differences in neutralizing activity for Omicron sub-lineages were observed between sera from Delta and Alpha breakthrough infections (Figure S1F), suggesting that neutralizing antibodies against the infected variant in breakthrough cases were not necessarily induced preferentially over neutralizing antibodies against other variants.

To understand the impact of viral replication in breakthrough infections on antibody response, we analyzed the relationship between upper respiratory viral load and neutralizing activity to each variant in the acute or convalescent phase (Figure 1C). In the acute phase, serum neutralization titers against ancestral strain and Alpha virus showed a significant negative correlation with upper respiratory viral load; similar trends were observed for acute phase serum neutralization titers against Delta virus; some serum neutralization titers against Beta, BA.1, BA.2, and BA.4/5 viruses in the acute phase were below detection limits, and precise correlations were not determined. However, convalescent phase serum-neutralizing titers against all variants correlated positively with upper respiratory viral load. Notably, the relationship between upper respiratory viral load and acute phase neutralization was exactly opposite to the relationship between upper respiratory viral load and convalescent phase neutralization. Moreover, the increase in neutralizing activity against all variants from the acute to convalescent phases (using paired sera) was strongly positive-correlated with the upper respiratory viral load (Figure 1D). This indicates that lower levels of neutralizing antibodies during the acute phase of breakthrough infections are associated with higher viral replication levels in the upper respiratory tract and that higher viral replication levels in the upper respiratory tract at the time of breakthrough infection induce a greater number of cross-neutralizing antibodies against a wide range of variants including Omicron variants in non-Omicron breakthrough infections.

### Cross-neutralizing activity

Previously, we reported that the cross-neutralizing activity of breakthrough convalescence sera against SARS-CoV-2 variants correlates with the vaccination-infection time interval.[7] However, the induction of antiviral immunity is expected to involve additional factors, including age, sex, symptomology, viral lineage, and viral replication. To explore the primary factors influencing neutralizing activity against each variant in breakthrough infections, we calculated correlation coefficients for each combination of factors: antibody titers, neutralization titers, age, sex, viral lineage (Delta, Alpha), viral load, the time interval from vaccination to infection, and the presence or absence of symptoms (Figure 2A). In the convalescent phase, all neutralization titers were strongly and positively correlated. Most neutralization titers were also positively correlated in the acute phase. However, neutralization titers in acute phase sera did not correlate with neutralization titers in the convalescent-phase sera for any variant (Figure 2A). This suggests that neutralizing activity in the acute phase does not determine subsequent antibody responses in the convalescent phase. Additionally, sex, age, and symptom onset showed no clear correlation with the neutralization titers in convalescent-phase sera. Delta variant infection was positively correlated with neutralization titers to ancestral and Beta viruses only, confirming the results shown above (Figure S1E). Conversely, the vaccination-infection interval was positively correlated with neutralization titers to ancestral, Beta, BA.1, BA.2, and BA.4/5 viruses in convalescent-phase sera. Additionally, upper respiratory viral load correlated strongly with the neutralization titers against all variants in convalescent-phase sera. This

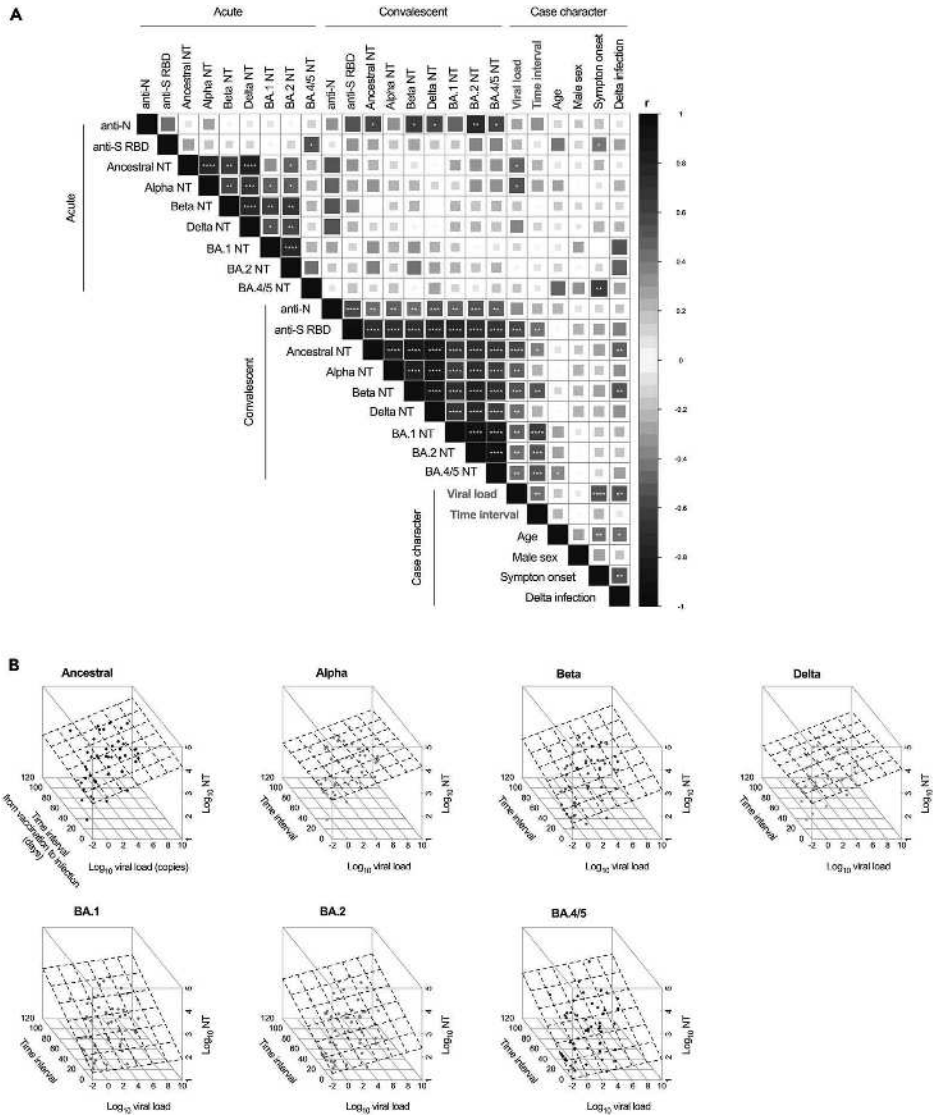


**Figure 2. Determinants of serum neutralization titers against SARS-CoV-2 variants in breakthrough infections**

(A) Spearman correlation matrix of antibody titers, viral load, and case characteristics for individuals with SARS-CoV-2 breakthrough infections. Neutralizing titers from pseudovirus neutralization tests, viral RNA copies used to represent viral load, and the time from vaccination to infection was employed herein. Male sex, disease onset, and Delta (vs. Alpha) variant infection were set as dummy variables (1 vs. 0). Spearman correlation r values were indicated using the square size and a heat scale. The statistical significance level, corrected using the false-discovery rate (FDR), is shown in the square; *p < 0.05, **p < 0.01, ***p < 0.001, ****p < 0.0001.

(B) Three-dimensional scatterplot of viral RNA load in respiratory specimens at a near-diagnosis date, the time interval from vaccination to infection, and neutralization titers against SARS-CoV-2 variants at the convalescent phase. The dotted planes represent regression planes. Table 1 shows the results of the multiple regression analysis relevant to the findings illustrated herein.

suggests that upper respiratory viral load at the time of diagnosis influences antibody responses in the convalescent phase following breakthrough infection.

To independently evaluate the impacts of these two different factors on neutralizing activity, we performed a multiple regression analysis on three parameters: neutralization titers for each variant, viral load, and the

**Table 1. Multiple regression analysis of neutralization titers, including viral load and the time interval from vaccination to infection**

| Pseudovirus | Variable | Coefficient | 95% CI | p-value |
|---|---|---|---|---|
| Ancestral ($log_{10}$ NT) | Time interval (d) | 0.003 | 0.011, −0.006 | 0.542 |
| | Viral load ($log_{10}$ copies) | 0.135 | 0.208, 0.062 | <0.001 |
| Alpha | Time interval | −0.002 | 0.008, −0.011 | 0.723 |
| | Viral load | 0.122 | 0.203, 0.042 | 0.004 |
| Beta | Time interval | 0.008 | 0.018, −0.001 | 0.077 |
| | Viral load | 0.123 | 0.202, 0.043 | 0.003 |
| Delta | Time interval | −0.002 | 0.008, −0.011 | 0.749 |
| | Viral load | 0.126 | 0.206, 0.045 | 0.003 |
| BA.1 | Time interval | 0.016 | 0.024, 0.008 | <0.001 |
| | Viral load | 0.049 | 0.118, −0.021 | 0.166 |
| BA.2 | Time interval | 0.012 | 0.021, 0.003 | 0.010 |
| | Viral load | 0.091 | 0.169, 0.014 | 0.022 |
| BA.4/5 | Time interval | 0.016 | 0.025, 0.007 | 0.001 |
| | Viral load | 0.067 | 0.146, −0.013 | 0.097 |

CI, confidence interval.

vaccination-infection time interval (Table 1). Further, we evaluated the slope coefficients for viral load and the vaccination-infection time interval on neutralization titers for each variant. The coefficients for viral load were significant for neutralization titers against ancestral, Alpha, Beta, Delta, and BA.2 viruses (but not for BA.1 or BA.4/5). However, although the coefficients for vaccination-infection time interval were significant for neutralization titers against BA.1, BA.2, and BA.4/5 viruses, they were not for the ancestral, Alpha, Beta, or Delta viruses. Moreover, three-dimensional plots utilizing neutralization titers to each variant, viral load, and the vaccination-infection time interval as independent variables revealed that the regression plane skewed more toward viral load in neutralizing activity to the ancestral strain, Alpha, and Delta, and more toward the vaccination-infection time interval in neutralizing activity to Beta, BA.1, BA.2, and BA.4/5 (Figure 2B). These results suggest that upper respiratory viral load more strongly determines convalescent phase neutralizing activity to ancestral, Alpha, Beta, and Delta viruses (vs. BA.1, BA.2, and BA.4/5). Contrarily, the vaccination-infection time interval more strongly determined the convalescent phase neutralizing activity to BA.1, BA.2, and BA.4/5. Two independent factors (upper respiratory viral load and the vaccination-infection time interval) showed differing magnitudes of impact for each variant on the induction of variant neutralizing antibodies in breakthrough infections.

### Antigenic distances

To better understand the overall picture regarding the potency of cross-neutralization, we performed antigenic cartography to locate the variants and sera in a two-dimensional map. Positions of variants and sera on antigenic maps were calculated based on each serum-neutralizing titer to each variant.[25,26] The antigenic distance between antigenically different variants is greater than that between antigenically similar variants.[27] Additionally, a shorter distance from serum to a variant on an antigenic map indicates higher neutralizing activity of the serum to the variant compared to other serum-variant pairs, meaning that sera with shorter variant-serum distances for many variants have higher cross-neutralizing activity. Thus, calculating the distance between each variant and serum on an antigenic map is useful for comparing the breadth of neutralizing activity for each serum. First, to evaluate how the antigenic distances between variants change depending on the immuno-history of the sera, an antigenic map was generated using serum-neutralizing titers to each variant obtained from individuals who were vaccinated twice (2vax) or three times (3vax) with BNT162b2 (the Pfizer/BioNTech mRNA vaccine) (Figures 3A and 3B). For 2vax sera, neutralization titers against Beta, BA.1, BA.2, and BA.4/5 were more than 10-fold lower than titers against ancestral strain (Figure 3A). The positions of each variant in 2vax sera were scattered on the antigenic map, with variants being spaced far apart (Figure 3B). Conversely, neutralization titers in 3vax sera against Beta, BA.1, and BA.2 variants were only reduced by around four times, and those against BA.4/5 were reduced by about nine times, compared to the ancestral strain (Figure 3A). Although BA.4/5 is the

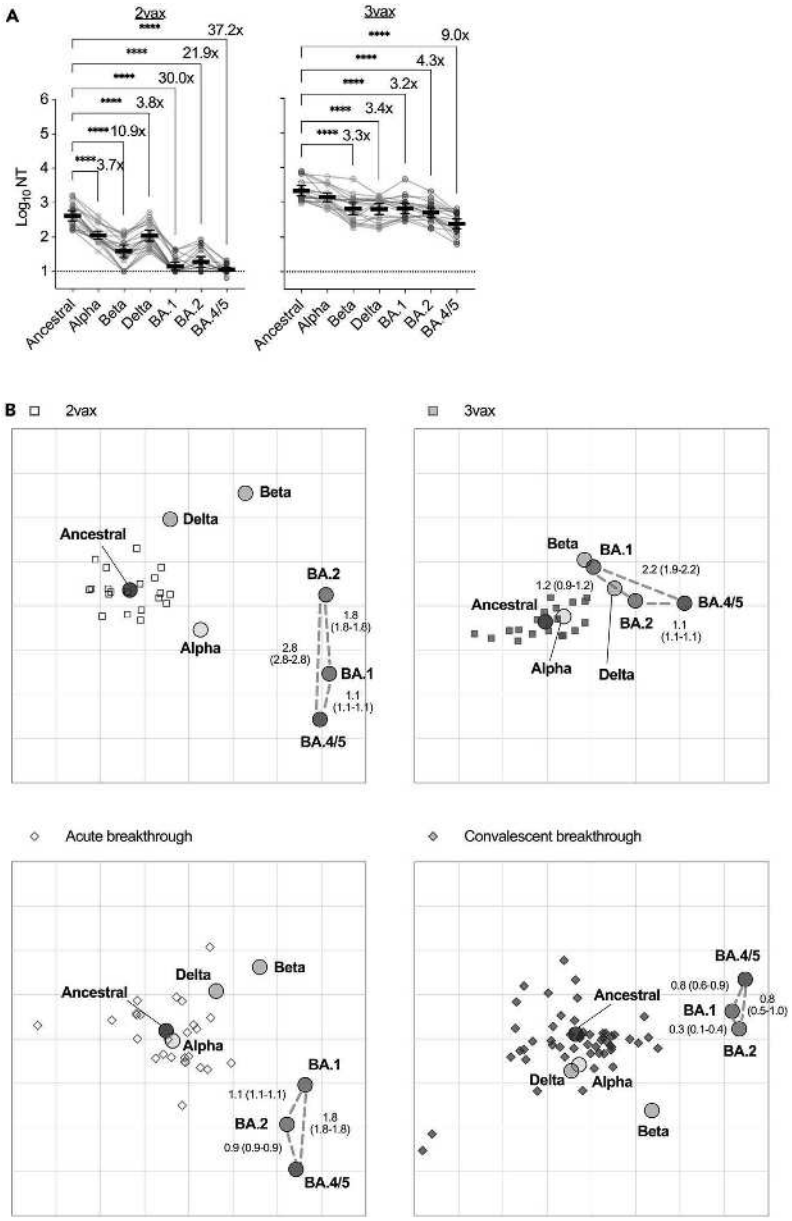


**Figure 3. Antigenic maps of SARS-CoV-2 variants for each serum source**

(A) Neutralization titers of sera obtained from individuals vaccinated twice (2vax) or three times (3vax) against variants of SARS-CoV-2 pseudoviruses. Data from the same serum are connected with lines, and the mean ±95% CIs of each serum titer are presented. The titers between the ancestral and newer variants were compared using one-way ANOVA with Dunnett's test; ****$p < 0.0001$. Fold reductions are indicated above columns given statistical significance. Dotted lines indicate cutoff values.

(B) Antigenic cartography of each serum source for the acute and convalescent phases of breakthrough infection, 2vax, and 3vax (against SARS-CoV-2 variants). The variants are shown as circles and sera are indicated as squares or diamonds. Each square and diamond corresponds to the sera of one individual; colors represent the serum source. Each grid square (1 antigenic unit) corresponds to a 2-fold dilution in the neutralization assay. Antigenic distance is interpretable in any direction. The median (interquartile range) of the distance among Omicron variants on the map is shown via gray dotted lines.

most antigenically distant from the ancestral strain, all variants including BA.4/5 were spaced close together compared to the map of 2vax sera (Figure 3B), suggesting that sera from individuals with booster dose vaccinations possess an expanded breadth of neutralizing activity against SARS-CoV-2 variants (including BA.1, BA.2, and BA.4/5) compared to those from individuals who were vaccinated twice. This result confirms that distances between each variant on the antigen map vary according to the nature of the sera used in the analysis. These results are consistent with the previously reported finding of a decrease in the antigenic distance between BA.1 and D614G variants in sera from booster vaccinees.[28]

Then, antigen maps were generated using acute phase or convalescent phase serum neutralization titers from individuals with breakthrough infections (Figure 3B). There were no obvious differences in the distances between the variants in the acute and convalescent phases of breakthrough infection, and there was more variation in the serum positions in both the acute and convalescent phases in breakthrough infections than in maps depicting 2vax and 3vax sera. This suggests that the breadth of neutralizing activity in breakthrough sera is as diverse from case to case as the magnitude of neutralizing activity. In contrast, the antigenic distances among BA.1, BA.2, and BA.4/5 in the map of the convalescent-phase sera were closer than those of other serum sources. This suggests that the convalescent sera contain robust neutralization potency against the amino acid changes introduced in the Omicron sub-lineages including BA.4/5.

### Vaccination-infection time interval and breadth of neutralizing activity

To compare the neutralizing breadth for each serum (obtained from vaccinees with or without breakthrough infection), an antigenic map was generated using 2vax, 3vax, and breakthrough infection sera simultaneously (Figure 4A). In this map, 3vax sera tended to be located closer to Beta, BA.1, BA.2, and BA.4/5 than 2vax sera (Figure 4A). We then calculated variant-serum distances between each serum and each variant. In the heatmap clustering individual variant-serum distances, Beta, BA.1, BA.2, and BA.4/5 were clustered in an antigenic group (antigenic group 2; vs. antigenic group 1, which included ancestral strain, Alpha, and Delta variants) (Figure 4B). This suggests that Beta, BA.1, BA.2, and BA.4/5 are antigenically distinct from ancestral strains. Additionally, almost all 3vax sera (but not 2vax sera) were classified as type 1 serum, with a short variant-serum distance for all variants (Figure 4B), suggesting that booster vaccination conferred a greater breadth of neutralizing activity against SARS-CoV-2 (including antigenically distinct variants). However, in breakthrough infection sera, neither acute nor convalescent-phase sera was classified into a specific serum type (Figure 4B), suggesting that the breadth of neutralizing activity in breakthrough infection was diversified from case to case.

Next, variant-serum distances were compared for 2vax, 3vax, acute phase, and convalescent-phase sera (Figure 4C). A shorter variant-serum distance indicated a higher degree of relative neutralization capacity of the serum to the variant. The variant-serum distances for the ancestral strain in 2vax, 3vax, acute phase, and convalescent-phase sera were shorter than those for the other variants and did not differ among serum sources. Conversely, variant-serum distances for antigenically distinct variants, such as Beta, BA.1, BA.2, and BA.4/5, were relatively longer than those for the ancestral, Alpha, and Delta variants. The variant-serum distances for 3vax, acute phase, and convalescent-phase sera (regarding the antigenically distinct variants) were statistically significantly shorter than for 2vax, suggesting that antibodies with an expanded breadth of neutralization covering antigenically distinct variants were induced in booster dose vaccinees, and in the acute/convalescent phases of breakthrough infection. Following this, we evaluated the impact of the infecting viral lineage on variant-serum distances and found no differences in the variant-serum distance in either the acute or the convalescent phase (Figure S2A). This suggests that the breadth of serum neutralization does not vary between Alpha and Delta breakthrough infections and that Alpha and Delta breakthrough infections (antigenic group 1) equally impact the extent of the breadth of neutralization against different antigenic variants (antigenic group 2).

Moreover, to assess the effect of the time interval on the breadth of neutralization, breakthrough sera were divided into short (early breakthrough) and long (late breakthrough) time interval groups, and variant-serum distances were compared for each variant and serum. The variant-serum distances for BA.1, BA.2, and BA.4/5 in the sera of the late breakthrough group were shorter than those in the early breakthrough group in the convalescent-phase sera (Figure S2B). Intriguingly, the variant-serum distance did not change between the early and late breakthrough groups for either variant in acute phase sera (Figure S2B). These observations suggest that the time interval from vaccination to infection strongly determines the breadth of neutralizing antibodies in the convalescent phase induced after breakthrough infection. We then evaluated

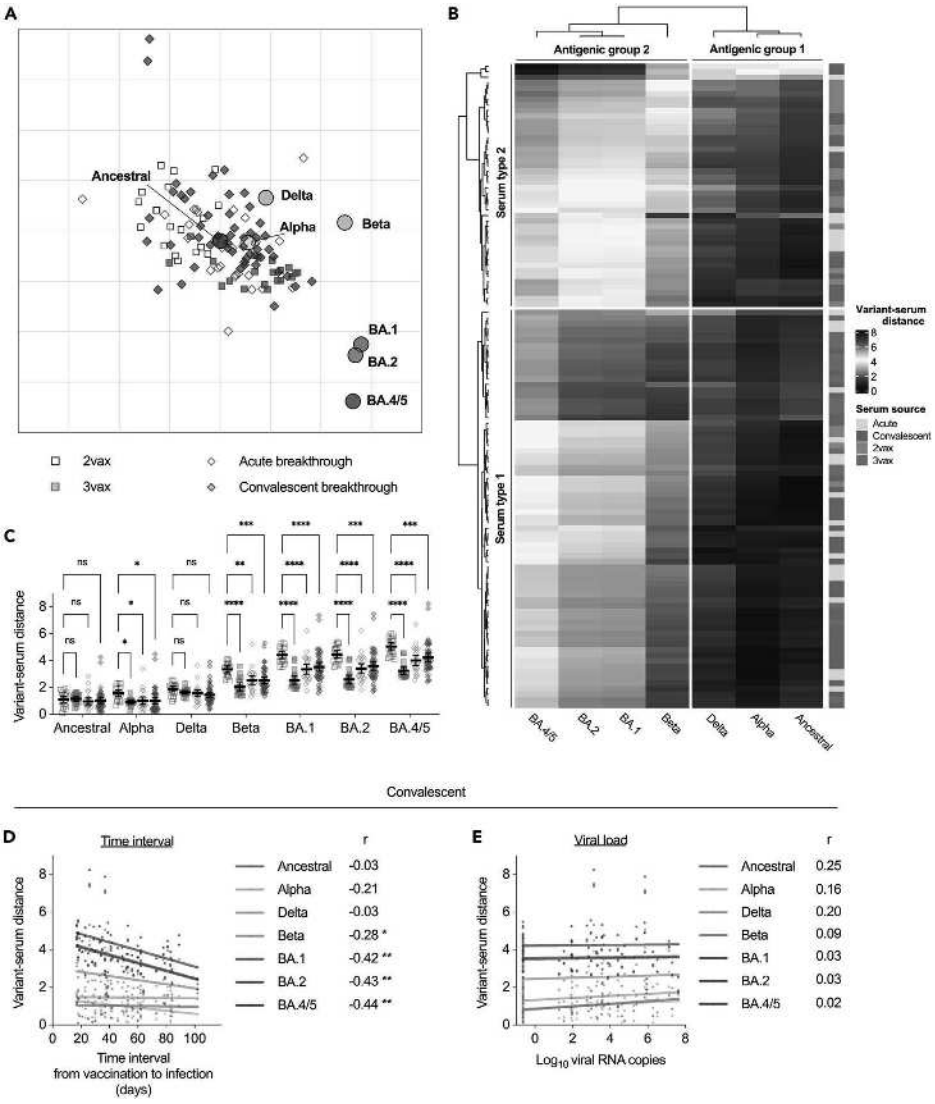


**Figure 4. Characterization of heterogeneous serum populations based on antigenic map distance, and sources of variation**

(A) Antigenic cartography of sera from acute/convalescent phases for breakthrough infections and for those receiving two (2vax) or three vaccines (3vax). Variants are shown as circles and sera are indicated as squares or diamonds. Each square or diamond corresponds to the sera of one individual; colors represent the serum source. Each grid square corresponds to a 2-fold dilution in the neutralization assay. Antigenic distance is interpretable in any direction.

(B) Clustering the antigenicity of SARS-CoV-2 variants and serum reactions against the variants. The heatmap shows the variant-serum distance from the sera. Two antigenic groups and three serum types were divided by k-means clustering. The serum sources are indicated by a color bar on the right.

(C) Comparison of variant-serum distance from the sera. Distances between the serum sources against 2vax sera were compared using two-way ANOVA with the Sidak test.

(D) Correlation between the time interval from vaccination to infection and variant-serum distance at the convalescent phase.

(E) Correlation between viral load in respiratory specimens at a near-diagnosis date and the variant-serum distance of sera at the convalescent phase. Statistical significance: ns, not significant, *$p < 0.05$, **$p < 0.01$, ***$p < 0.001$, ****$p < 0.0001$.

the correlation between variant-serum distances in breakthrough infection sera, the vaccination-infection time interval, and the upper respiratory viral load (Figures 4D and 4E). Variant-serum distances for the ancestral, Alpha, and Delta variants did not correlate with the vaccination-infection time interval, while the variant-serum distances for antigenically distinct variants correlated negatively. Upper respiratory viral load did not correlate with variant-serum distances for any variants. These results suggest that the vaccination-infection time interval acts as a primary determinant of variant-serum distances for antigenically distinct variants from the vaccine antigen and ancestral strain without being limited by the antigenicity of the infecting virus or viral replication and that a longer time interval contributes to expanding the breadth of neutralization regarding antigenically distinct variants.

### Neutralizing activity of anti-spike IgG antibodies

Finally, the relationship among the amount of anti-spike IgG antibodies in breakthrough infection sera, neutralization titer, time interval, and upper respiratory viral load was examined (Figure S3). IgG antibody levels binding to Omicron BA.1 spike were approximately 6-fold lower than those to the ancestral spike in the acute and convalescent sera (Figure S3A). However, IgG antibody levels binding to other variant spikes were comparable to those to the ancestral spike (Figure S3A). Then, we evaluated the correlation among these anti-spike IgG levels, neutralizing titers, the time interval, and the viral load (Figure S3B). In the convalescent sera, anti-spike IgG antibody levels were highly, positively correlated with neutralizing titers for all variants (Figures S3B and S3C). However, in acute phase sera, anti-spike IgG antibody levels showed no clear correlation with neutralizing titers for any of the variants (Figures S3B and S3C). These results suggest that in breakthrough infections, anti-spike IgG antibodies induced in the convalescent phase after infection have higher neutralizing activity than the IgG antibodies in sera collected immediately after infection, and immune responses induced after breakthrough infections promote the production of more potent anti-spike antibodies Then, we calculated the neutralizing titer per anti-spike IgG antibody amount and evaluated the correlation with time interval and viral load (Figure S3D). Neutralizing activity per spike-binding IgG antibody against Beta and BA.1 variant was highly correlated with time interval. Taken together, these results suggest that the neutralizing potency of individual spike-binding IgG antibodies to antigenically distinct variants improve with increasing time interval.

## DISCUSSION

COVID-19-vaccine breakthrough infections were previously found to elicit robust cross-neutralizing antibody responses against several SARS-CoV-2 variants, which were largely recalled from memory B cells induced by previous vaccinations.[29] Vaccination-infection time interval effect on cross-neutralizing antibody responses may also be due to antibody affinity maturation as a result of the accumulation of somatic mutations in memory B cells and positive/negative selection in the germinal center (GC).[30] The SARS-CoV-2 mRNA vaccine was reported to induce a GC response that is strongly associated with the induction of SARS-CoV-2 binding antibodies and memory B cells.[31,32] The GC response lasted at least 12 weeks after the second doses of the vaccine, enabling the generation of robust humoral immunity.[32] Memory B cells recognizing Omicron and other variants are known to proliferate after the second vaccination[33,34] and memory B cells recognizing the Omicron spike proliferate after the third vaccination.[33] These findings support the contention that a third exposure increases the B cell population producing antibodies with high cross-neutralizing potency. Indeed, affinity maturation of IgG antibodies to the spike-protein-conserved region persisted for more than three months after SARS-CoV-2 infection in a prior study.[30] Furthermore, cross-neutralization ability against antigenically distant variants was induced in a group with a longer first-to-second vaccination interval.[32] Our results and previous findings support the importance of the time interval between vaccinations in the progression of the breadth of neutralization potency to SARS-CoV-2 regarding both booster vaccinations and breakthrough infections.

Moreover, we showed that the upper respiratory viral load in Delta or Alpha (i.e., antigenic group 1) breakthrough-infected individuals correlated with the resulting increase in the magnitude of the neutralization potency to SARS-CoV-2, including variants belonging to antigenic group 2 (Figure 1). This finding indicates that the viral replication level in the upper respiratory tract impacts neutralizing antibody production. It has been reported in non-human primate infectious models and observational studies on COVID-19 vaccine breakthrough infections that low levels of neutralizing antibodies prior to infection allow for efficient viral replication in the upper respiratory tract.[35–37] This is consistent with the present results showing an obvious relationship between acute-phase neutralizing activity and viral load. It has also been reported that lower viral load in the upper respiratory tract tends to induce more neutralizing

antibodies in unvaccinated SARS-CoV-2-infected patients,[38] which is contrary to the present results showing a positive relationship between convalescent phase neutralizing activity and viral load in breakthrough infections. This suggests that the induction of neutralizing antibodies in breakthrough infections involves an interaction between pre-existing immunity obtained through vaccination and viral replication during breakthrough infection. Viral replication can modulate antiviral immunity by synthesizing viral antigens that serve as immunogens for inducing antiviral antibodies. Intriguingly, the effect of upper respiratory viral load on neutralizing antibody production in Delta/Alpha variant breakthrough infections was seen for both antigenically similar variants (ancestral, Alpha, and Delta variants) and antigenically distinct variants (Beta, BA.1, BA.2, BA.4/5) across the antigenic barrier. This suggests that viral antigens supplied by upper respiratory viral replication in breakthrough infected cases might be sufficient to overcome the antigenic barrier by stimulating B cells against neutralizing epitopes that are conserved among variants including antigenically distinct Omicron variants only in individuals infected after a sufficient time interval. In addition, it is noteworthy that both high and low levels of cross-neutralizing antibodies to BA.4 and BA.5 have been reported in cases of breakthrough infections.[14–18] This indicates that some specific conditions are required for the induction of broad immunity covering BA.4 and BA.5 after breakthrough infections, supporting our hypothesis. Furthermore, the hypothesis implies the potential for a different approach to rational antigen design in booster vaccine development aimed at inducing a broad breadth of protective immunity (i.e., covering all SARS-CoV-2 variants). The time interval rather than the upper respiratory viral load was shown to expand the breadth of neutralization. However, further evaluation of the impact of upper respiratory viral load on the expansion of neutralization breadth in breakthrough infections with antigenically distinct viruses relative to the current vaccine strain is needed to fully elucidate the role of viral replication as a key driver of upgrading neutralizing activity in individuals with breakthrough infections.

In conclusion, we found that non-Omicron breakthrough infections elicited robust cross-neutralizing activity against Omicron variants (including BA.4/5 sub-lineage) across the antigenic barrier. Most importantly, our findings clearly demonstrated that the length of the post-vaccination incubation period, but not the antigenicity of the infecting virus or the upper respiratory viral load, is a critical determinant in expanding the breadth of neutralization to antigenically distinct variants. Additionally, the upper respiratory virus load at the time of infection is associated with the amount of neutralizing antibody titer produced during the subsequent convalescent phases. Respiratory viral load and the vaccination-infection time interval each showed a variable magnitude of impact for each variant in regard to the induction of neutralizing antibodies in breakthrough-infected individuals. Consequently, antiviral immunity to SARS-CoV-2 is becoming increasingly diverse in individuals with breakthrough infections. Therefore, exploratory studies evaluating factors controlling the quality of the immune response after breakthrough infection can be a useful guide for the development of next-generation vaccines with the ability to induce a durable and broad breadth of protective immunity against all SARS-CoV-2 variants. This study highlights the importance of dosing interval optimization to develop a variant-proof booster vaccine.[1]

### Limitations of the study

Despite the overall strengths of this study, it has several limitations. First, the cases enrolled in this study were limited to breakthrough cases infected with the Alpha or Delta variants and did not include cases infected with the Omicron variant. Due to an increase in the population who have a longer time interval between vaccination and infection, infections during the Omicron pandemic may lead to the development of more potent cross-neutralizing antibodies.[17,18] Second, the disease severity of the breakthrough cases enrolled in this study was predominantly biased toward asymptomatic and mild cases. However, COVID-19 disease severity is reported to be an important determinant of antibody induction in unvaccinated individuals.[30,38] Third, since acute phase sera from individuals with breakthrough infections showed a low neutralization titer (even against the ancestral virus) in our investigation, we could not determine an accurate fold reduction in the neutralizing antibody titer or an accurate correlation coefficient against respiratory viral load. Fourth, we did not assess T-cell immunity and Fc-effector function in humoral immunity, such as antibody-dependent cellular cytotoxicity (ADCC) and antibody-dependent cellular phagocytosis (ADCP), which may be associated with vaccine efficacy.[37,39–41] Fifth, no individual who experienced breakthrough infection after the booster dose was enrolled in this study. Sixth, breakthrough infection sera for individuals' vaccination-infection time intervals of more than four months were not available in this study, and the interval that maximizes cross-neutralization potency remains unknown. Seventh, the accurate antigen placement in standard antigenic cartography requires each

variant-infected serum.[25] However, since this study focused on the relative placement of variant antigens and sera in the different immune histories of vaccinated and breakthrough-infected sera, Omicron-infected sera were not necessarily required. Finally, our investigation did not evaluate the actual risk of reinfection by SARS-CoV-2 in individuals with a history of breakthrough infection, although there is evidence that neutralizing antibody titers can be a correlate of protection against ancestral strains and different variants.[42–44]

It should be noted that control of upper respiratory viral replication in breakthrough cases is more difficult to achieve than control of the vaccination-infection time interval, as viral replication in the respiratory tract is influenced by multiple variables, including the infecting variant, amount of viral exposure, host susceptibility, treatment strategies (including antiviral drugs), innate immune response, and complex pre-existing acquired immunity to SARS-CoV-2. For this, inducing high-quality antiviral immunity against SARS-CoV-2 following breakthrough infections is difficult to control. Therefore, breakthrough infection should not be considered an option for boosting immunity.

## STAR★METHODS

Detailed methods are provided in the online version of this paper and include the following:

- KEY RESOURCES TABLE
- RESOURCE AVAILABILITY
  - Lead contact
  - Material availability
  - Data and code availability
- EXPERIMENTAL MODEL AND SUBJECT DETAILS
  - Human participants and sampling
  - Ethical approval
  - Cells
  - SARS-CoV-2 virus
- METHOD DETAILS
  - RNA extraction and RT-qPCR
  - SARS-CoV-2 viral RNA genome sequencing
  - PCR screening for mutation detection
  - Viral isolation and titration
  - VSV pseudovirus production
  - Electrochemiluminescence immunoassay (ECLIA)
  - VSV pseudovirus-based neutralization assay
  - Live virus neutralization assay
- QUANTIFICATION AND STATISTICAL ANALYSIS
  - Antigenic cartography
  - Statistical analysis

## SUPPLEMENTAL INFORMATION

Supplemental information can be found online at https://doi.org/10.1016/j.isci.2023.105969.

## ACKNOWLEDGMENTS

We thank Akiko Sataka, Asato Kojima, Izumi Kobayashi, Yuki Iwamoto, Yuko Sato, Milagros Virhuez Mendoza, Noriko Nakajima, Kenta Takahashi, and Emi Taeda at the National Institute of Infectious Diseases (NIID) for their technical support and Fukumi Nakamura-Uchiyama at Tokyo Metropolitan Bokutoh Hospital and Hidefumi Shimizu at JCHO Tokyo Shinjuku Medical Center for the collection of blood samples from vaccinees. We also thank the healthcare facilities, local health centers, and public health institutes for their contribution in providing us with valuable patient information and samples on breakthrough cases as listed previously.[7] We also thank GISAID for the platform to share and compare our data with data submitted globally. This work was supported by a Japanese Society for the Promotion of Science Grants-in-Aid for Scientific Research (JSPS KAKENHI) grant 21K20768 (to S Miyamoto) and by Japan Agency for Medical Research and Development (AMED) grants JP21fk0108104 (to TS), JP22fk0108637 (to TS), JP22fk0108141 (to TS), JP20fk0108534 (to YT), and JP21fk0108615 (to YT).

## AUTHOR CONTRIBUTIONS

Conceptualization, S Miyamoto, TA, TS; methodology, S Miyamoto, TA, AU, TK, SS, H Katano, SI, S Moriyama, SF, YT, TS; investigation, S Miyamoto, TA, AU, TK, SS, H Katano, SI, AA, SO, TH, YH, S Moriyama, RK, H Kinoshita, SY, MS, SF; data curation, S Miyamoto, TA, TS, S Moriyama, RK, MS; formal analysis, S Miyamoto, TS; Visualization, S Miyamoto; funding acquisition, S Miyamoto, YT, TS; project administration, TS; supervision, TS; writing original draft, S Miyamoto, TS; writing – review & editing, S Miyamoto, TA, AU, TK, SS, H Katano, SI, AA, TH, YH, S Moriyama, RK, H Kinoshita, SY, MS, SF, YT, TS. All authors agreed to submit the article, read and approved the final draft, and take full responsibility for its content including the accuracy of the data and statistical analysis.

## DECLARATION OF INTERESTS

The authors declare no competing interests.

Received: July 15, 2022
Revised: December 31, 2022
Accepted: January 9, 2023
Published: February 17, 2023

## REFERENCES

1. Dolgin, E. (2022). Pan-coronavirus vaccine pipeline takes form. Nat. Rev. Drug Discov. *21*, 324–326. https://doi.org/10.1038/d41573-022-00074-6.

2. Carreño, J.M., Alshammary, H., Tcheou, J., Singh, G., Raskin, A.J., Kawabata, H., Sominsky, L.A., Clark, J.J., Adelsberg, D.C., Bielak, D.A., et al. (2022). Activity of convalescent and vaccine serum against SARS-CoV-2 Omicron. Nature *602*, 682–688. https://doi.org/10.1038/s41586-022-04399-5.

3. Cele, S., Jackson, L., Khoury, D.S., Khan, K., Moyo-Gwete, T., Tegally, H., San, J.E., Cromer, D., Scheepers, C., Amoako, D.G., et al. (2022). Omicron extensively but incompletely escapes Pfizer BNT162b2 neutralization. Nature *602*, 654–656. https://doi.org/10.1038/s41586-021-04387-1.

4. Dejnirattisai, W., Shaw, R.H., Supasa, P., Liu, C., Stuart, A.S., Pollard, A.J., Liu, X., Lambe, T., Crook, D., Stuart, D.I., et al. (2022). Reduced neutralisation of SARS-CoV-2 omicron B.1.1.529 variant by post-immunisation serum. Lancet *399*, 234–236. https://doi.org/10.1016/S0140-6736(21)02844-0.

5. Garcia-Beltran, W.F., St. Denis, K.J., Hoelzemer, A., Lam, E.C., Nitido, A.D., Sheehan, M.L., Berrios, C., Ofoman, O., Chang, C.C., Hauser, B.M., et al. (2022). mRNA-based COVID-19 vaccine boosters induce neutralizing immunity against SARS-CoV-2 Omicron variant. Cell *185*, 457–466.e4. https://doi.org/10.1016/j.cell.2021.12.033.

6. Schmidt, F., Muecksch, F., Weisblum, Y., Da Silva, J., Bednarski, E., Cho, A., Wang, Z., Gaebler, C., Caskey, M., Nussenzweig, M.C., et al. (2022). Plasma neutralization of the SARS-CoV-2 omicron variant. N. Engl. J. Med. *386*, 599–601. https://doi.org/10.1056/NEJMc2119641.

7. Miyamoto, S., Arashiro, T., Adachi, Y., Moriyama, S., Kinoshita, H., Kanno, T., Saito, S., Katano, H., Iida, S., Ainai, A., et al. (2022). Vaccination-infection interval determines cross-neutralization potency to SARS-CoV-2 Omicron after breakthrough infection by other variants. Med *3*, 249–261.e4. https://doi.org/10.1016/j.medj.2022.02.006.

8. Servellita, V., Syed, A.M., Morris, M.K., Brazer, N., Saldhi, P., Garcia-Knight, M., Sreekumar, B., Khalid, M.M., Ciling, A., Chen, P.-Y., et al. (2022). Neutralizing immunity in vaccine breakthrough infections from the SARS-CoV-2 Omicron and Delta variants. Cell *185*, 1539–1548.e5. https://doi.org/10.1016/j.cell.2022.03.019.

9. Walls, A.C., Sprouse, K.R., Bowen, J.E., Joshi, A., Franko, N., Navarro, M.J., Stewart, C., Cameroni, E., McCallum, M., Goecker, E.A., et al. (2022). SARS-CoV-2 breakthrough infections elicit potent, broad, and durable neutralizing antibody responses. Cell *185*, 872–880.e3. https://doi.org/10.1016/j.cell.2022.01.011.

10. Wratil, P.R., Stern, M., Priller, A., Willmann, A., Almanzar, G., Vogel, E., Feuerherd, M., Cheng, C.-C., Yazici, S., Christa, C., et al. (2022). Three exposures to the spike protein of SARS-CoV-2 by either infection or vaccination elicit superior neutralizing immunity to all variants of concern. Nat. Med. *28*, 496–503. https://doi.org/10.1038/s41591-022-01715-4.

11. Iketani, S., Liu, L., Guo, Y., Liu, L., Chan, J.F.W., Huang, Y., Wang, M., Luo, Y., Yu, J., Chu, H., et al. (2022). Antibody evasion properties of SARS-CoV-2 Omicron sublineages. Nature *604*, 553–556. https://doi.org/10.1038/s41586-022-04594-4.

12. Seki, Y., Yoshihara, Y., Nojima, K., Momose, H., Fukushi, S., Moriyama, S., Wagatsuma, A., Numata, N., Sasaki, K., Kuzuoka, T., et al. (2022). Safety and immunogenicity of the Pfizer/BioNTech SARS-CoV-2 mRNA third booster vaccine dose against the SARS-CoV-2 BA.1 and BA.2 Omicron variants. Med *3*, 406–421.e4. https://doi.org/10.1016/j.medj.2022.04.013.

13. Yu, J., Collier, A.-r.Y., Rowe, M., Mardas, F., Ventura, J.D., Wan, H., Miller, J., Powers, O., Chung, B., Siamatu, M., et al. (2022). Neutralization of the SARS-CoV-2 omicron BA.1 and BA.2 variants. N. Engl. J. Med. *386*, 1579–1580. https://doi.org/10.1056/NEJMc2201849.

14. Cao, Y., Yisimayi, A., Jian, F., Song, W., Xiao, T., Wang, L., Du, S., Wang, J., Li, Q., Chen, X., et al. (2022). BA.2.12.1, BA.4 and BA.5 escape antibodies elicited by Omicron infection. Nature *608*, 593–602. https://doi.org/10.1038/s41586-022-04980-y.

15. Hachmann, N.P., Miller, J., Collier, A.-r.Y., Ventura, J.D., Yu, J., Rowe, M., Bondzie, E.A., Powers, O., Surve, N., Hall, K., and Barouch, D.H. (2022). Neutralization escape by SARS-CoV-2 omicron subvariants BA.2.12.1, BA.4, and BA.5. N. Engl. J. Med. *387*, 86–88. https://doi.org/10.1056/NEJMc2206576.

16. Tuekprakhon, A., Huo, J., Nutalai, R., Dijokaite-Guraliuc, A., Zhou, D., Ginn, H.M., Selvaraj, M., Liu, C., Mentzer, A.J., Supasa, P., et al. (2022). Antibody escape of SARS-CoV-2 Omicron BA.4 and BA.5 from vaccine and BA.1 serum. Cell *185*, 2422–2433.e13. https://doi.org/10.1016/j.cell.2022.06.005.

17. Qu, P., Faraone, J., Evans, J.P., Zou, X., Zheng, Y.-M., Carlin, C., Bednash, J.S., Lozanski, G., Mallampalli, R.K., Saif, L.J., et al. (2022). Neutralization of the SARS-CoV-2 omicron BA.4/5 and BA.2.12.1 subvariants. N. Engl. J. Med. *386*, 2526–2528. https://doi.org/10.1056/NEJMc2206725.

18. Quandt, J., Muik, A., Salisch, N., Lui, B.G., Lutz, S., Krüger, K., Wallisch, A.-K., Adams-Quack, P., Bacher, M., Finlayson, A., et al. (2022). Omicron BA.1 breakthrough infection drives cross-variant neutralization and memory B cell formation against conserved epitopes. Sci. Immunol. *7*, eabq2427. https://doi.org/10.1126/sciimmunol.abq2427.

19. Tober-Lau, P., Gruell, H., Vanshylla, K., Koch, W.M., Hillus, D., Schommers, P., Suárez, I., Suttorp, N., Sander, L.E., Klein, F., and Kurth, F. (2022). Cross-variant neutralizing serum activity after SARS-CoV-2 breakthrough infections. Emerg. Infect. Dis. *28*, 1050–1052. https://doi.org/10.3201/eid2805.220271.

20. Chatterjee, D., Tauzin, A., Marchitto, L., Gong, S.Y., Boutin, M., Bourassa, C., Beaudoin-Bussières, G., Bo, Y., Ding, S., Laumaea, A., et al. (2022). SARS-CoV-2 Omicron Spike recognition by plasma from individuals receiving BNT162b2 mRNA vaccination with a 16-week interval between doses. Cell Rep. *38*, 110429. https://doi.org/10.1016/j.celrep.2022.110429.

21. Hall, V.G., Ferreira, V.H., Wood, H., Ierullo, M., Majchrzak-Kita, B., Manguiat, K., Robinson, A., Kulasingam, V., Humar, A., and Kumar, D. (2022). Delayed-interval BNT162b2 mRNA COVID-19 vaccination enhances humoral immunity and induces robust T cell responses. Nat. Immunol. *23*, 380–385. https://doi.org/10.1038/s41590-021-01126-6.

22. Tauzin, A., Gong, S.Y., Beaudoin-Bussières, G., Vézina, D., Gasser, R., Nault, L., Marchitto, L., Benlarbi, M., Chatterjee, D., Nayrac, M., et al. (2022). Strong humoral immune responses against SARS-CoV-2 Spike after BNT162b2 mRNA vaccination with a 16-week interval between doses. Cell Host Microbe *30*, 97–109.e5. https://doi.org/10.1016/j.chom.2021.12.004.

23. Bortz, E., Westera, L., Maamary, J., Steel, J., Albrecht, R.A., Manicassamy, B., Chase, G., Martínez-Sobrido, L., Schwemmle, M., and García-Sastre, A. (2011). Host- and strain-specific regulation of influenza virus polymerase activity by interacting cellular proteins. mBio *2*, e00151-11. https://doi.org/10.1128/mBio.00151-11.

24. Li, B., Deng, A., Li, K., Hu, Y., Li, Z., Shi, Y., Xiong, Q., Liu, Z., Guo, Q., Zou, L., et al. (2022). Viral infection and transmission in a large, well-traced outbreak caused by the SARS-CoV-2 Delta variant. Nat. Commun. *13*, 460. https://doi.org/10.1038/s41467-022-28089-y.

25. Smith, D.J., Lapedes, A.S., de Jong, J.C., Bestebroer, T.M., Rimmelzwaan, G.F., Osterhaus, A.D.M.E., and Fouchier, R.A.M. (2004). Mapping the antigenic and genetic evolution of influenza virus. Science *305*, 371–376. https://doi.org/10.1126/science.1097211.

26. Wilks, S. (2021). Racmacs: R antigenic cartography macros. https://github.com/acorg/Racmacs.

27. Mykytyn, A.Z., Rissmann, M., Kok, A., Rosu, M.E., Schipper, D., Breugem, T.I., van den Doel, P.B., Chandler, F., Bestebroer, T., de Wit, M., et al. (2022). Omicron BA.1 and BA.2 are antigenically distinct SARS-CoV-2 variants. Preprint at bioRxiv. https://doi.org/10.1101/2022.02.23.481644.

28. Lusvarghi, S., Pollett, S.D., Neerukonda, S.N., Wang, W., Wang, R., Vassell, R., Epsi, N.J., Fries, A.C., Agan, B.K., Lindholm, D.A., et al. (2022). SARS-CoV-2 BA.1 variant is neutralized by vaccine booster-elicited serum, but evades most convalescent serum and therapeutic antibodies. Sci. Transl. Med. *14*, eabn8543. https://doi.org/10.1126/scitranslmed.abn8543.

29. Bates, T.A., McBride, S.K., Winders, B., Schoen, D., Trautmann, L., Curlin, M.E., and Tafesse, F.G. (2022). Antibody response and variant cross-neutralization after SARS-CoV-2 breakthrough infection. JAMA *327*, 179–181. https://doi.org/10.1001/jama.2021.22898.

30. Moriyama, S., Adachi, Y., Sato, T., Tonouchi, K., Sun, L., Fukushi, S., Yamada, S., Kinoshita, H., Nojima, K., Kanno, T., et al. (2021). Temporal maturation of neutralizing antibodies in COVID-19 convalescent individuals improves potency and breadth to circulating SARS-CoV-2 variants. Immunity *54*, 1841–1852.e4. https://doi.org/10.1016/j.immuni.2021.06.015.

31. Lederer, K., Bettini, E., Parvathaneni, K., Painter, M.M., Agarwal, D., Lundgreen, K.A., Weirick, M., Muralidharan, K., Castaño, D., Goel, R.R., et al. (2022). Germinal center responses to SARS-CoV-2 mRNA vaccines in healthy and immunocompromised individuals. Cell *185*, 1008–1024.e15. https://doi.org/10.1016/j.cell.2022.01.027.

32. Turner, J.S., O'Halloran, J.A., Kalaidina, E., Kim, W., Schmitz, A.J., Zhou, J.Q., Lei, T., Thapa, M., Chen, R.E., Case, J.B., et al. (2021). SARS-CoV-2 mRNA vaccines induce persistent human germinal centre responses. Nature *596*, 109–113. https://doi.org/10.1038/s41586-021-03738-2.

33. Goel, R.R., Painter, M.M., Apostolidis, S.A., Mathew, D., Meng, W., Rosenfeld, A.M., Lundgreen, K.A., Reynaldi, A., Khoury, D.S., Pattekar, A., et al. (2021). mRNA vaccines induce durable immune memory to SARS-CoV-2 and variants of concern. Science *374*, abm0829. https://doi.org/10.1126/science.abm0829.

34. Kotaki, R., Adachi, Y., Moriyama, S., Onodera, T., Fukushi, S., Nagakura, T., Tonouchi, K., Terahara, K., Sun, L., Takano, T., et al. (2022). SARS-CoV-2 Omicron-neutralizing memory B-cells are elicited by two doses of BNT162b2 mRNA vaccine. Sci. Immunol. *7*, eabn8590. https://doi.org/10.1126/sciimmunol.abn8590.

35. Arunachalam, P.S., Walls, A.C., Golden, N., Atyeo, C., Fischinger, S., Li, C., Aye, P., Navarro, M.J., Lai, L., Edara, V.V., et al. (2021). Adjuvanting a subunit COVID-19 vaccine to induce protective immunity. Nature *594*, 253–258. https://doi.org/10.1038/s41586-021-03530-2.

36. Bergwerk, M., Gonen, T., Lustig, Y., Amit, S., Lipsitch, M., Cohen, C., Mandelboim, M., Levin, E.G., Rubin, C., Indenbaum, V., et al. (2021). Covid-19 breakthrough infections in vaccinated health care workers. N. Engl. J. Med. *385*, 1474–1484. https://doi.org/10.1056/NEJMoa2109072.

37. McMahan, K., Yu, J., Mercado, N.B., Loos, C., Tostanoski, L.H., Chandrashekar, A., Liu, J., Peter, L., Atyeo, C., Zhu, A., et al. (2021). Correlates of protection against SARS-CoV-2 in rhesus macaques. Nature *590*, 630–634. https://doi.org/10.1038/s41586-020-03041-6.

38. Wang, Y., Zhang, L., Sang, L., Ye, F., Ruan, S., Zhong, B., Song, T., Alshukairi, A.N., Chen, R., Zhang, Z., et al. (2020). Kinetics of viral load and antibody response in relation to COVID-19 severity. J. Clin. Invest. *130*, 5235–5244. https://doi.org/10.1172/JCI138759.

39. Richardson, S.I., Madzorera, V.S., Spencer, H., Manamela, N.P., van der Mescht, M.A., Lambson, B.E., Oosthuysen, B., Ayres, F., Makhado, Z., Moyo-Gwete, T., et al. (2022). SARS-CoV-2 Omicron triggers cross-reactive neutralization and Fc effector functions in previously vaccinated, but not unvaccinated, individuals. Cell Host Microbe *30*, 880–886.e4. https://doi.org/10.1016/j.chom.2022.03.029.

40. Rostad, C.A., Chen, X., Sun, H.y., Hussaini, L., Lu, A., Perez, M.A., Hsiao, H.M., Anderson, L.J., and Anderson, E.J. (2022). Functional antibody responses to severe acute respiratory syndrome coronavirus 2 variants in children with coronavirus disease 2019, multisystem inflammatory syndrome in children, and after two doses of BNT162b2 vaccination. J. Infect. Dis. *226*, 1237–1242. https://doi.org/10.1093/infdis/jiac215.

41. Zhu, D.Y., Gorman, M.J., Yuan, D., Yu, J., Mercado, N.B., McMahan, K., Borducchi, E.N., Lifton, M., Liu, J., Nampanya, F., et al. (2022). Defining the determinants of protection against SARS-CoV-2 infection and viral control in a dose-down Ad26.CoV2.S vaccine study in nonhuman primates. PLoS Biol. *20*, e3001609. https://doi.org/10.1371/journal.pbio.3001609.

42. Cromer, D., Steain, M., Reynaldi, A., Schlub, T.E., Wheatley, A.K., Juno, J.A., Kent, S.J., Triccas, J.A., Khoury, D.S., and Davenport, M.P. (2022). Neutralising antibody titres as predictors of protection against SARS-CoV-2 variants and the impact of boosting: a meta-analysis. Lancet Microbe *3*, e52–e61. https://doi.org/10.1016/S2666-5247(21)00267-6.

43. Feng, S., Phillips, D.J., White, T., Sayal, H., Aley, P.K., Bibi, S., Dold, C., Fuskova, M., Gilbert, S.C., Hirsch, I., et al. (2021). Correlates of protection against symptomatic and asymptomatic SARS-CoV-2 infection. Nat. Med. *27*, 2032–2040. https://doi.org/10.1038/s41591-021-01540-1.

44. Gilbert, P.B., Montefiori, D.C., McDermott, A.B., Fong, Y., Benkeser, D., Deng, W., Zhou, H., Houchens, C.R., Martins, K., Jayashankar, L., et al. (2022). Immune correlates analysis of the mRNA-1273 COVID-19 vaccine efficacy clinical trial. Science *375*, 43–50. https://doi.org/10.1126/science.abm3425.

45. Tani, H., Kimura, M., Tan, L., Yoshida, Y., Ozawa, T., Kishi, H., Fukushi, S., Saijo, M., Sano, K., Suzuki, T., et al. (2021). Evaluation of SARS-CoV-2 neutralizing antibodies using a vesicular stomatitis virus possessing SARS-CoV-2 spike protein. Virol. J. *18*, 16. https://doi.org/10.1186/s12985-021-01490-7.

46. Shirato, K., Nao, N., Katano, H., Takayama, I., Saito, S., Kato, F., Katoh, H., Sakata, M., Nakatsu, Y., Mori, Y., et al. (2020). Development of genetic diagnostic methods for detection for novel coronavirus 2019(nCoV-2019) in Japan. Jpn. J. Infect. Dis. *73*, 304–307. https://doi.org/10.7883/yoken.JJID.2020.061.

47. Takahashi, K., Ishikane, M., Ujiie, M., Iwamoto, N., Okumura, N., Sato, T., Nagashima, M., Moriya, A., Suzuki, M., Hojo, M., et al. (2022). Duration of infectious virus shedding by SARS-CoV-2 omicron variant–infected vaccinees. Emerg. Infect. Dis. *28*, 998–1001. https://doi.org/10.3201/eid2805.220197.

48. Itokawa, K., Sekizuka, T., Hashino, M., Tanaka, R., and Kuroda, M. (2020). Disentangling primer interactions improves SARS-CoV-2 genome sequencing by multiplex tiling PCR. PLoS One *15*, e0239403. https://doi.org/10.1371/journal.pone.0239403.

49. Yamada, S., Fukushi, S., Kinoshita, H., Ohnishi, M., Suzuki, T., Fujimoto, T., Saijo, M., and Maeda, K.; Virus Diagnosis Group NIID Toyama (2021). Assessment of SARS-CoV-2 infectivity of upper respiratory specimens from COVID-19 patients by virus isolation using VeroE6/TMPRSS2 cells. BMJ Open Respir. Res. *8*, e000830. https://doi.org/10.1136/bmjresp-2020-000830.

50. Matsuyama, S., Nao, N., Shirato, K., Kawase, M., Saito, S., Takayama, I., Nagata, N., Sekizuka, T., Katoh, H., Kato, F., et al. (2020). Enhanced isolation of SARS-CoV-2 by TMPRSS2-expressing cells. Proc. Natl. Acad. Sci. USA *117*, 7001–7003. https://doi.org/10.1073/pnas.2002589117.

51. Mathew, D., Giles, J.R., Baxter, A.E., Oldridge, D.A., Greenplate, A.R., Wu, J.E., Alanio, C., Kuri-Cervantes, L., Pampena, M.B., D'Andrea, K., et al. (2020). Deep immune profiling of COVID-19 patients reveals distinct immunotypes with therapeutic implications. Science *369*, eabc8511. https://doi.org/10.1126/science.abc8511.

## STAR★METHODS

### KEY RESOURCES TABLE

| REAGENT or RESOURCE | SOURCE | IDENTIFIER |
|---|---|---|
| Bacterial and virus strains | | |
| hCoV-19/Japan/TY-WK-521/2020 | National Institute of Infectious Diseases | EPI_ISL_408667 |
| hCoV-19/Japan/QHN002/2020 | National Institute of Infectious Diseases | EPI_ISL_804008 |
| hCoV-19/Japan/TY8-612/2021 | National Institute of Infectious Diseases | EPI_ISL_1123289 |
| hCoV-19/Japan/TY11-927-P1/2021 | National Institute of Infectious Diseases | EPI_ISL_2158617 |
| hCoV-19/Japan/TY38-873P0/2021 | National Institute of Infectious Diseases | EPI_ISL_7418017 |
| hCoV-19/Japan/TY40-158-P0/2022 | National Institute of Infectious Diseases | EPI_ISL_9595813 |
| hCoV-19/Japan/TY41-702-P1/2022 | National Institute of Infectious Diseases | EPI_ISL_13241867 |
| VSV pseudovirus bearing SARS-CoV-2 spike protein | Tani et al.[45] | N/A |
| Biological samples | | |
| Human plasma samples obtained from vaccinated health care workers | Tokyo Shinagawa Hospital | N/A |
| Human serum samples obtained from breakthrough cases | Miyamoto et al.[7] | N/A |
| Human respiratory specimens | This paper | N/A |
| Critical commercial assays | | |
| Bright-Glo Luciferase Assay System | Promega | E2620 |
| V-PLEX SARS-CoV-2 Panel 23 Kit | Meso Scale Discovery | K15567U-2 |
| Elecsys Anti-SARS-CoV-2 (200) RUO | Roche Diagnostics | 518316181 |
| Elecsys Anti-SARS-CoV-2 S (200) RUO | Roche Diagnostics | 518316488 |
| QuantiTect Probe RT-PCR Kit | Qiagen | 204445 |
| QIAseq FX DNA Library Kit | Qiagen | 180473 |
| Experimental models: Cell lines | | |
| VeroE6/TMPRSS2 cells | JCRB Cell Bank | JCRB1819 |
| Oligonucleotides | | |
| NIID-N2 primer/probe set | Shirato et al.[46] | N/A |
| N501Y detection primers: 5′- CTTGTAATGGTGTTRAA GGTTTTAATTGT 5′- GGTGCA TGTAGAAGTTCAAAAGAAAG | This paper | N/A |
| Probes for N501 detection: 5′-FAM-CCAACACCATTAGT GGGTTG-MGB; for 501Y detection: 5′-VIC- CCAACACCATAAGTGGGTTG-MGB | This paper | N/A |
| L452R detection primers: 5′-GCGTTATAGCTTGGAATT CTAACAATC 5′- ATCTCTCTC AAAAGGTTTGAGATTAGAC | This paper | N/A |
| Probes for L452 detection: 5′-FAM-ATTATAATTACCTGT ATAGATTGT-MGB; for 452R detection: 5′- VIC-TTATAATTACCGGTATAGATTG-MGB | This paper | N/A |
| Primer/probe for E484K | Takara | RC345A |

(Continued on next page)

*Continued*

| REAGENT or RESOURCE | SOURCE | IDENTIFIER |
|---|---|---|
| Software and algorithms | | |
| Graphpad Prism 9 | Graphpad | N/A |
| R 4.1.2 | R Core Team | https://www.R-project.org/ |
| Racmacs | Wilks[26] | https://github.com/acorg/Racmacs |
| Other | | |
| GroMax Navigator Microplate Luminometer | Promega | GM2000 |
| MESOQuickPlex SQ 120 | Meso Scale Discovery | AI0AA-0 |
| cobas e 411 plus | Roche Diagnostics | N/A |
| MiSeq System | Illumina | SY-410-1003 |

## RESOURCE AVAILABILITY

### Lead contact

Additional information and requests for resources and reagents should be directed to the lead contact, Tadaki Suzuki (tksuzuki@niid.go.jp).

### Material availability

SARS-CoV-2 viruses in this study are available from the National Institute of Infectious Diseases (NIID) under a material transfer agreement with the NIID, Tokyo, Japan.

### Data and code availability

All data are available in the main text or the supplemental information.

This study did not generate any new codes.

Any additional information required to reanalyze the data reported in this work paper is available from the lead contact upon request.

## EXPERIMENTAL MODEL AND SUBJECT DETAILS

### Human participants and sampling

The characteristics of human participants included in this study are summarized in Table S1. Human plasma samples obtained from vaccinated healthcare workers with no infections who received two or three doses of BNT162b2 (Pfizer/BioNTech) mRNA vaccine were collected with written informed consent prior to enrollment and ethics approval by the medical research ethics committee of the NIID. Blood obtained from vaccinated health care workers was collected in Vacutainer cell preparation tubes (CPT; BD Biosciences, Franklin Lakes, NJ, US) and centrifuged at 1,800 × g for 20 min. Peripheral blood mononuclear cells (PBMCs) were suspended in plasma and harvested into conical tubes, followed by centrifugation at 300 × g for 15 min. The plasma was then transferred into another conical tube and centrifuged at 800 × g for 15 min, and the supernatant was transferred into another tube to completely remove PBMCs.

Human serum samples obtained from breakthrough cases were also included in this study. A breakthrough infection was defined according to a positive result in a test detecting SARS-CoV-2 RNA or antigen conducted on a respiratory specimen collected ≥14 days after the second vaccine dose. Demographic information, vaccination status, and respiratory samples for determining the infecting variant in the breakthrough cases included in this report were collected as part of the public health activity led by NIID under the Infectious Diseases Control Law and were published on the NIID website in order to meet statutory requirements. Sera obtained from breakthrough cases were collected concurrently for clinical testing provided by the NIID (with patient consent), and neutralization assays for this report were performed using residual samples as a research activity with ethics approval from the medical research ethics committee of NIID and informed consent.

We considered cases with positive anti-N antibody titers in the acute phase to have a history of pre-existing infection. To examine neutralization, plasma and serum samples were heat-inactivated at 56°C for 30 min before use. The median dose interval between the first and second vaccine dose for both vaccinated uninfected individuals and breakthrough cases was 21 days (Table S1).

Respiratory specimens were collected through nasal swabs, nasopharyngeal swabs, or saliva samples. Quantitative reverse transcriptase polymerase chain reaction (RT-qPCR) assays were completed at NIID for all respiratory samples to confirm sample quality for genome sequencing and to quantify the viral RNA load.

### Ethical approval

All samples, protocols, and procedures described herein were approved by the Medical Research Ethics Committee of NIID for involving human participants (approval numbers 1178, 1275, 1316, and 1321).

### Cells

HEK293T cells obtained from the American Type Culture Collection (Manassas, VA, USA) were cultured in Dulbecco's modified Eagle medium (DMEM; Fujifilm, Tokyo, Japan) supplemented with 10% fetal bovine serum (FBS) at 37°C, and were supplied with 5% $CO_2$. VeroE6/TMPRSS2 cells (JCRB1819, Japanese Collection of Research Bioresources Cell Bank; Osaka, Japan) were maintained in low glucose DMEM (Fujifilm) containing 10% heat-inactivated FBS (Biowest, Nuaillé, France), 1 mg/mL geneticin (Thermo Fisher Scientific), and 100 U/mL penicillin/streptomycin (Thermo Fisher Scientific) at 37°C; these cells were supplied with 5% $CO_2$.

### SARS-CoV-2 virus

We used the SARS-CoV-2 ancestral strain WK-521 (lineage A, GISAID ID: EPI_ISL_408667) and the Omicron BA.2 variant TY40-158 (lineage BA.2.3, EPI_ISL_9595813) in this study; these variants were isolated using VeroE6/TMPRSS2 cells at NIID with ethics approval provided by the medical research ethics committee of NIID for studies conducted with human subjects (#1178). More specifically, to isolate viruses belonging to the Omicron BA.2 variant TY40-158 strain, respiratory specimens collected from individuals screened at airport quarantine stations in Japan and transferred to NIID for whole genome sequencing were subjected to viral isolation using VeroE6/TMPRSS2 cells at NIID.

## METHOD DETAILS

### RNA extraction and RT-qPCR

RNA was extracted from respiratory samples using the Maxwell RSC miRNA Plasma and Serum kit (Promega, Madison, WI, USA). Quantification cycle (Cq) values (i.e., viral RNA loads) were measured by RT-qPCR using the QuantiTect Probe RT-PCR Kit (Qiagen, Hilden, Germany) targeting the SARS-CoV-2 nucleoprotein (N) region via an NIID-N2 primer/probe set.[46] The thermal cycling conditions were as follows: 50°C for 30 min; 95°C for 15 min; and 45 cycles of 95°C for 15 s and 60°C for 1 min. The Cq values of samples judged to be negative were analyzed by substituting a Cq value of 45. Cq values were converted to viral nucleoprotein RNA copy numbers/reaction according to a previously reported simple regression line.[47] Viral isolation and PCR screening for mutations of interest (N501Y, E484K, L452R) were attempted for NIID-N2 primer/probe set positive samples.

### SARS-CoV-2 viral RNA genome sequencing

For respiratory specimens with Cq values of less than 32, SARS-CoV-2 whole viral genome sequences were determined. A primer set modified from the ARTIC Network's V1 primer set (https://github.com/ItokawaK/Alt_nCov2019_primers/tree/master/Primers/ver_N3) was used for conducting multiplex RT-PCR. A DNA library was constructed from the RT-PCR products using the QIAseq FX DNA Library Kit (Qiagen) as described previously,[48] and was subjected to next-generation sequencing using the MiSeq System (Illumina, San Diego, CA, USA). Consensus sequences of the viral genome were obtained using the ARTIC field bioinformatics pipeline, following the ARTIC-nCoV-bioinformatics SOP-v1.1.0 (https://artic.network/ncov-2019/ncov2019-bioinformatics-sop.html, 2020). The consensus sequences were uploaded to the Global Initiative on Sharing All Influenza Data (GISAID; https://www.gisaid.org/).

### PCR screening for mutation detection

To support genome sequencing analysis to determine variants, PCR screening for N501Y, E484K, and L452R mutations was completed for all RT-qPCR positive samples. Two in-house PCR assays to detect N501Y and L452R mutations, respectively, had previously been developed at NIID for public health surveillance purposes. To screen for N501Y mutations in the spike (S) region, we designed primers [5′- CTTG TAATGGTGTTRAAGGTTTTAATTGT and 5′- GGTGCATGTAGAAGTTCAAAAGAAAG] and TaqMan MGB probes [for N501 detection: 5′-FAM-CCAACACCATTAGTGGGTTG-MGB; for 501Y detection: 5′-VIC- CCAACACCATAAGTGGGTTG-MGB]. To detect L452R mutations in the S domain, we likewise designed primers [5′-GCGTTATAGCTTGGAATTCTAACAATC and 5′- ATCTCTCTCAAAAGGTTTGAGAT TAGAC] and TaqMan MGB probes [for L452 detection: 5′-FAM-ATTATAATTACCTGTATAGATTGT-MGB; for 452R detection: 5′- VIC-TTATAATTACCGGTATAGATTG-MGB]. The final concentrations of the primers and probes were 0.6 μM and 0.1 μM, respectively. The reagents and the reaction conditions for RT-qPCR were as described above. For the E484K mutation, a commercial primer/probe for E484K (Takara, Kusatsu, Japan) was used.

We defined SARS-CoV-2 variants as follows: (i) Alpha lineage, samples in which E484 and 501Y were detected; (ii) Delta lineage, samples in which the 452R was detected; and (iii) undetermined, samples in which the 484K was detected or mutation detections failed. There were no discordant results for these PCR assays in regard to viral genome sequencing in included cases until August 2021.

### Viral isolation and titration

Viral isolation was attempted for all RT-qPCR positive cases with available residual respiratory specimens, as described previously.[49] Briefly, VeroE6/TMPRSS2 cells[50] (JCRB1819, JCRB Cell Bank) were seeded in 96-well flat-bottom plates, respiratory specimens mixed with DMEM supplemented with 2% FBS and Antibiotic-Antimycotic Solution (Thermo Fisher Scientific) were inoculated in duplicate, and the culture supernatant was changed to fresh medium one day post-infection (d.p.i.) and was incubated at 37°C and supplied with 5% $CO_2$. On one and five d.p.i., a cytopathic effect was observed. After five days, the supernatant was collected and RT-qPCR using the SARS-CoV-2 direct detection RT-qPCR kit (Takara) was performed in order to confirm the propagation of SARS-CoV-2. The median tissue culture infectious dose ($TCID_{50}$) in the residual specimens was determined for all viral isolation positive cases.

### VSV pseudovirus production

The vesicular stomatitis virus (VSV) pseudovirus bearing SARS-CoV-2 spike protein was generated as previously described.[45] Briefly, the spike genes of SARS-CoV-2 ancestral, Alpha, Beta, Delta, Omicron BA.1, BA.4/5 variants were obtained from viral RNA extracted from the SARS-CoV-2 WK-521 strain (ancestral strain), QHN002 (Alpha; lineage B.1.1.7, GISAID: EPI_ISL_804008), TY8-612 (Beta; lineage B.1.351, GISAID: EPI_ISL_1123289), TY11-927 (Delta; lineage B.1.617.2, GISAID: EPI_ISL_2158617), TY38-873 (lineage BA.1, GISAID: EPI_ISL_7418017), and TY41-702 (lineage BA.5, GISAID: EPI_ISL_13241867) respectively, by RT-PCR (PrimeScript II High Fidelity One Step RT-PCR Kit, Takara). The spike genes of the SARS-CoV-2 Omicron variants were obtained from RNA extracted from nasopharyngeal swab specimens from patients infected with the SARS-CoV-2 Omicron BA.2 variant (TY40-158) by RT-PCR, as described above. The cytoplasmic 19 aa-deleted SARS-CoV-2 spike genes were cloned into a pCAGGS/MCS expression vector. HEK293T cells transfected with expression plasmids encoding the SARS-CoV-2 spike genes for the ancestral, Alpha, Beta, Delta, BA.1, BA.2, and BA.4/5 variants were infected with G-complemented VSVΔG/Luc. After 24 h, the culture supernatants containing VSV pseudoviruses were collected and stored at −80°C until further use.

### Electrochemiluminescence immunoassay (ECLIA)

Antibody titers for the ancestral spike (S) receptor binding domain (RBD) and nucleoprotein (N) were measured using Elecsys Anti-SARS-CoV-2 S (Roche, Basel, Switzerland) and Elecsys Anti-SARS-CoV-2 S (Roche) kits according to manufacturer instructions. Anti-spike IgG antibody levels for variants were measured using V-PLEX SARS-CoV-2 Panel 23 Kit (Meso Scale Discovery) according to the manufacturer's instructions.

### VSV pseudovirus-based neutralization assay

Neutralization of SARS-CoV-2 pseudoviruses was performed as described previously.[7,29] Briefly, serially diluted serum (with five-fold serial dilution of serum from participants with second vaccinations, or eight-fold serial dilution of serum from breakthrough infected patients and participants with third vaccinations, starting at a 1:10 dilution) was mixed with an equal volume of VSV pseudovirus-bearing SARS-CoV-2 spike protein and incubated at 37°C for 1 h. The mixture was then inoculated into VeroE6/TMPRSS2 cells seeded on 96-well solid white flat-bottom plates (Corning; Corning, NY, USA). At 24 h post-infection, the infectivity of the VSV pseudovirus was assessed by measuring luciferase activity using a Bright-Glo Luciferase Assay System (Promega) and a GloMax Navigator Microplate Luminometer (Promega). The reciprocal half-maximal inhibitory dilution ($ID_{50}$) is presented as the serum neutralization titer.

### Live virus neutralization assay

Live virus neutralization assays were performed as described previously.[7,29] Briefly, serum samples were serially diluted (via two-fold dilutions starting from 1:5) in high-glucose DMEM supplemented with 2% FBS and 100 U/mL penicillin/streptomycin and were mixed with 100 $TCID_{50}$ SARS-CoV-2 viruses (WK-521, ancestral strain; and TY40-158, Omicron BA.2 variant), followed by incubation at 37°C for 1 h. The virus-serum mixtures were placed on VeroE6/TMPRSS2 cells seeded in 96-well plates and cultured at 37°C with 5% $CO_2$ for five days. After culturing, the cells were fixed with 20% formalin (Fujifilm) and stained with crystal violet solution (Sigma-Aldrich, St. Louis, MO, USA). Neutralization titers were defined as the geometric mean of the reciprocal of the highest sample dilution that protects at least 50% of the cells from a cytopathic effect from two to four multiplicate series. Since sera from individuals who suffered from breakthrough infections were limited in quantity, this assay was performed only once. All experiments using authentic viruses were performed in a biosafety level 3 laboratory at NIID.

## QUANTIFICATION AND STATISTICAL ANALYSIS

### Antigenic cartography

Antigenic maps based on neutralization titers against SARS-CoV-2 pseudoviruses were created using the *Racmacs* R function (The R Project for Statistical Computing, Vienna, Austria) with 2,000 optimizations.[25,26] Each grid square (1 antigenic unit) corresponded to a two-fold dilution in the neutralization assay. Antigenic distance (i.e., map distance) was used as the variant-serum distance (https://acorg.github.io/Racmacs/articles/intro-to-antigenic-cartography.html). Medians and interquartile ranges of the distances between BA.1, BA.2, and BA.4/5 variants were calculated by Pythagorean theorem using the coordinates of antigenic maps in optimization steps. Heatmaps were created to visualize variant-serum distances using the *ComplexHeatmap* R function.

### Statistical analysis

Data analysis and visualization were performed using GraphPad Prism 9.3.1 (San Diego, CA, USA) and R 4.1.2. Measurements below the detection limit, excluding Cq values, were converted to half the detection limit. For statistical analysis, unpaired t-tests, one-way analysis of variance (ANOVA) with Dunnett's test, and two-way ANOVA with the Sidak test were used to compare viral loads, antibody titers, and variant-serum distances. Pearson correlation coefficients were used to assess correlations between continuous variables. Statistical significance was set at $p < 0.05$. In correlation matrix analyses, Spearman correlations between variables were calculated with false discovery rate (FDR) correction and were visualized using the *psych* and *corrplot* R functions, as described previously.[51] Coefficients were indicated using square size and the aforementioned heat scale.

In multiple regression analysis, each neutralization antibody titer against ancestral and newer SARS-CoV-2 variants in convalescent sera was regressed against respiratory viral load ($x_1$, viral RNA copies) at a near-diagnosis date as well as the time interval ($x_2$, days) from vaccination to infection. The model for neutralization titer $y$ for participant $i$ can be written as follows:

$$\mathrm{Log}_{10}\, y_i = \beta_0 + \beta_1 \log_{10} x_{1i} + \beta_2 x_{2i} + \varepsilon_i$$

$\beta_0$ represents the $y$-intercept; and $\beta_1$, $\beta_2$, and $\varepsilon$ represent the slope coefficients and error term, respectively. These analyses and visualizations were performed using the *stats* and *scatterplot3d* R functions.